

Developments and Applications of TRACE/CFD Model of

Maanshan PWR Pressure Vessel

Yu-Ting Ku¹, Yung-Shin Tseng¹, Jung-Hua Yang¹
Shao-Wen Chen², Jong-Rong Wang^{2,3}, and Chunkuan Shin^{2,3}

¹: Department of Engineering and System Science, National Tsing Hua University,
No. 101, Section 2, Kuang-Fu Rd., Hsinchu, Taiwan, R.O.C.

²: Institute of Nuclear Engineering and Science, National Tsing Hua University,
No. 101, Section 2, Kuang-Fu Rd., Hsinchu, Taiwan, R.O.C.

³: Nuclear and New Energy Education and Research Foundation,
No. 101, Section 2, Kuang-Fu Rd., Hsinchu, Taiwan, R.O.C.
s100011801@m100.nthu.edu.tw

ABSTRACT

In this study, a three-dimensional PWR pressure vessel model has been developed using the CFD and TRACE codes to simulate the flow behaviors and thermal-hydraulic phenomena in the downcomer and lower-plenum of Maanshan PWR nuclear power plant. Detailed geometries of vessel components such as neutron shield panels, core support, lower core plate, butt-type columns were considered in this model for flow calculations. Important settings of the present CFD model were first validated with the test data from ROCOM facility. Following those settings and considering the geometries and operating conditions of Maanshan NPP, the CFD model of Maanshan PWR pressure vessel was first built for steady-state simulations and prepared for transient accident analyses.

In order to provide sufficient transient boundary conditions for transient CFD simulations, the TRACE Maanshan model was coupled with the present CFD pressure vessel model. In this study, main steam line break accident (MSLB) was chosen as a transient event for simulations and analyses. It was found that unexpected temperature and pressure variations can be found in vessel within a short period. In addition, the locations of loop inlets and the neutron shielding plate in downcomer may affect the core flow distributions and enhance core cooling rate in some parts of pressure vessel. This study demonstrated that a methodology of TRACE/CFD model for Maanshan PWR pressure vessel has been successfully developed, and the present simulation results and analyses can be used for reactor safety analyses and further transient applications.

KEYWORDS

CFD, PWR, FLUENT, TRACE, MSLB

1. INTRODUCTION

There are two methods to confirm whether the nuclear power plants (NPP) would operate in safety environment or not, by experimentation and by safety analysis. In this paper, the main steamline break (MSLB) transient in Maanshan PWR was performed by safety analysis, which provides numerous simulation data for estimating the operational margin in different conditions. In PWR, the heat transfer effect and flow mixing phenomenon have significant effects on MSLB. In order to study these flow

behaviors, this paper established a reactor pressure vessel (RPV) model by using Communication CFD code FLUENT[1]. The thermal hydraulic data obtained from FLUENT calculation could be feedback to other code, especially as system code with one-dimensional or simplification three-dimensional vessel module calculation, to improve the accuracy of thermal hydraulic simulation.

Maanshan NPP is the third NPP and the only PWR in Taiwan. The object of this study is to develop and apply the Maanshan vessel module to MSLB transient analysis. The Maanshan vessel module was developed according to the real NPP design with sensible simplification and the NPP operating data as module boundary condition. ROCOM, Rossendorf coolant mixing model experiment, is a final summary report about the test matrix on flow distribution and the steady state mixing with different various mass flow rates [2,3]. To validate the credibility of Maanshan vessel module, the important coefficients and simulation methods had been compared with ROCOM experimental data. And the results verify that the module has an ability to analyze the Maanshan vessel.

2. GEOMETRICAL MODEL AND MESH GENERATION

During the development of Maanshan NPP CFD module, doing the verifications of meshing scheme, numerical method and turbulence model we selected is necessary. ROCOM is the proper case for these verifications because the geometry of ROCOM experiment facility is similar to Maanshan vessel. In order to find the appropriate meshing scheme, numerical method and turbulence model, we established the ROCOM CFD model by using FLUENT and verified it by ROCOM experimental data. Because of the geometric similarity between ROCOM experiment facility and Maanshan vessel, the methods used during ROCOM CFD model construction were also applied in Maanshan CFD module. According to these verifications, the appropriate meshing scheme, numerical method and turbulence model would be choose and used in Maanshan NPP CFD module.

2.1. ROCOM Experiment AND CFD model

Figure 1 shows the ROCOM test facility. The ROCOM facility is a KONVO type reactor in a linear scale of 1:5, consisting of a pressure vessel, four working loops, wire-mesh sensors and two water tanks. Each working loop has an individually controllable pump to perform flow conditions tests. The flow leaves the vessel from hot legs and is percolated in water tank, and then it would go back to working loop. For the measurement and investigation of flow mixing phenomenon, the material of vessel shell chooses transparent acryl. The wire-mesh sensors could measure the transient tracer concentration in both space domain and time domain. The coolant flow is injected into downcomer via cold legs, and the detail flow information is detected by wire-mesh sensors in downcomer. In addition, at each fuel assembly inlet, there are sensors.

ROCOM CFD module was constructed according to the test facility design, as shown in figure 2. For saving the calculation time, the reasonable simplification of module utilized in this module is listed below :

- a) water tanks and pumps were ignored as constant cold leg inlet;
- b) vessel outlet were replaced by fuel assembly inlet.

The initial conditions (Table 1) of ROCOM-STAT 01 test was selected as boundary conditions in ROCOM CFD module, and the results from ROCOM-STAT 01 test was used to verify the ROCOM CFD module.

2.2. Maanshan CFD model

A three-dimensional Maanshan vessel model, including only downcomer and lower plenum, had been built by using CFD code FLUENT (Fig. 3), and utilized to understand the thermal hydraulic behavior and mixing phenomenon. The vessel model, according to real NPP design, consists of cold legs, hot legs, neutron shield panels, core support, lower core plate, butt type columns, energy absorber assembly, upper tie-plate, lower tie-plate and secondly core support.

In order to converge the model and save the computational time, some assumptions and simplifications was employed to develop the geometrical model in this research:

- Upper plenum and core were ignored because FLUENT cannot do the neutron kinetic calculation. For the same reason, model outlet was changed from hot legs to lower core plate.
- In order to compensate for the decrease of flow resistance, because of the simplification above, a porous zone was added at outlet.
- The wall in this CFD model was considered as adiabatic for prevent heat loss while we calculate the flow mixing.

Moreover, an unstructured mesh system was employed to generate meshes in this model (Fig. 3). The mesh was roughly about 9.52 million cells with tetrahedron/ hexahedral/ wedge meshes, and the maximum mesh skewness was controlled below 0.93. The computer with Intel core i5, 16GB RAM and Windows 7 operating system was used in this paper. The execution time for the ROCOM CFD analysis was about 24 hours and for the Maanshan CFD analysis was about 2 weeks.

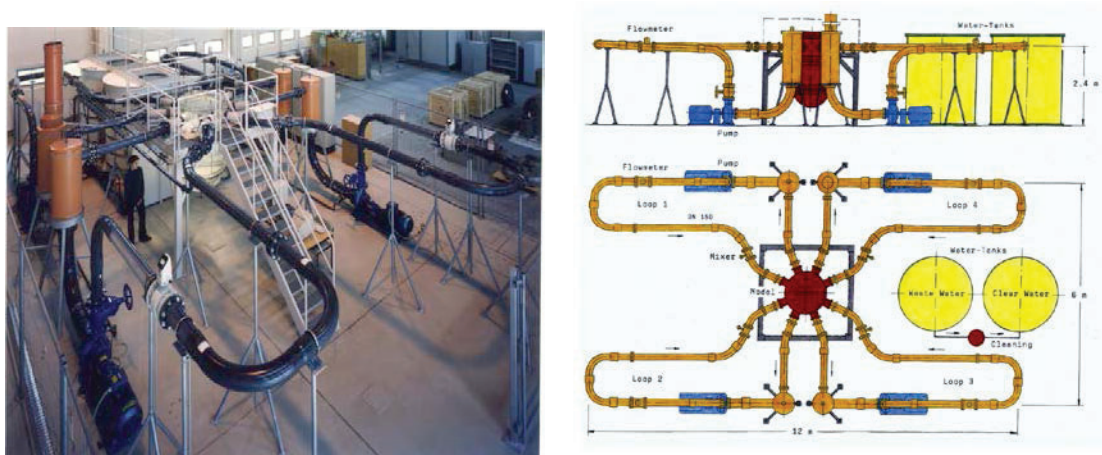


Figure 1. Acryl model of the RPV and frame view on the ROCOM test facility

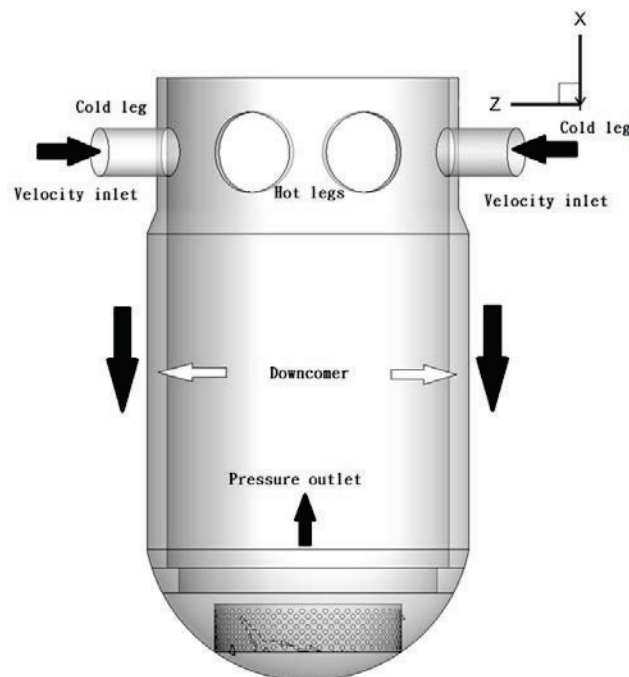


Figure 2. ROCOM CFD model

Table 1. Flow rate at cold-leg inlet of each loop

| Run | Flow rate [m ³ /h] | | | |
|---------------|-------------------------------|--------|--------|--------|
| | Loop 1 | Loop 2 | Loop 3 | Loop 4 |
| ROCOM-STAT 01 | 185 | 185 | 185 | 184 |

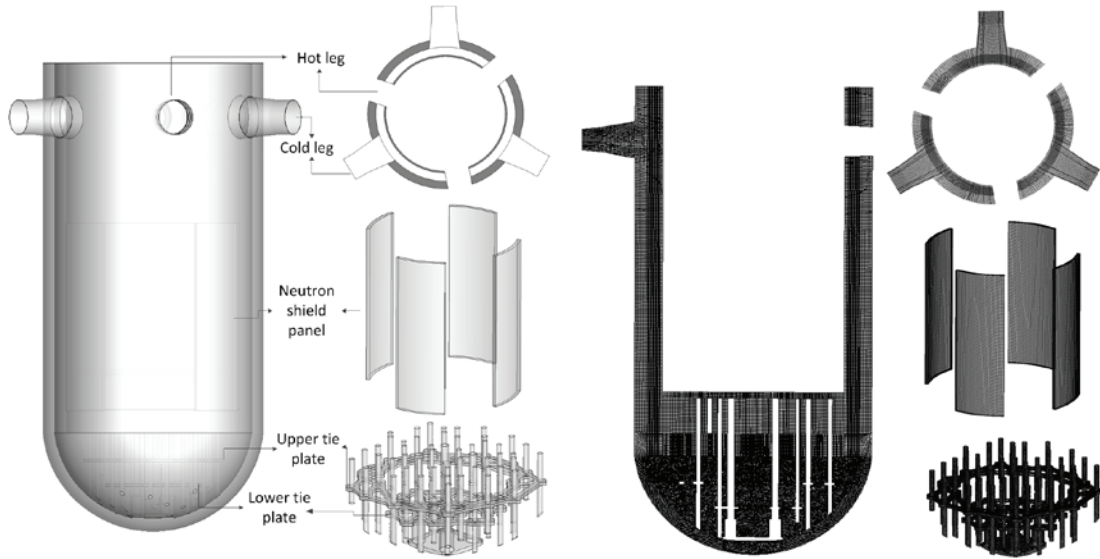


Figure 3. Maanshan simulation model and mesh distribution

2.3. Maanshan TRACE model

The steady-state and transient-state calculations were performed in this paper. In steady state, the operating data of Maanshan NPP was utilized as boundary condition of Maanshan CFD model. In transient state, the event with obvious temperature drop, such as Main Steam Line Break accident (MSLB), was used to provide extreme temperature variation to investigate the temperature mixing effect of flow field. MSLB, a design basis accident, was selected as transient event. In MSLB transient, high pressure coolant injection (HPI) and low pressure coolant injection (LPI) were assumed to be failure, and only accumulator (ACC) injection was available.

The result of unnormal MSLB transient was provided by Maanshan TRACE model [4,5]. TRACE is a system code for NPP safety analysis. Maanshan TRACE model has three feedwater control system loops, including the pressure vessel, pressurizer, steam generators, steam piping at the secondary side, the accumulators, and safety injection of ECCS [6,7]. In addition, the Maanshan TRACE model had been verified by Maanshan NPP startup test report (Fig. 4). Setting parameter and boundary conditions in this case were based on NPP operating data.

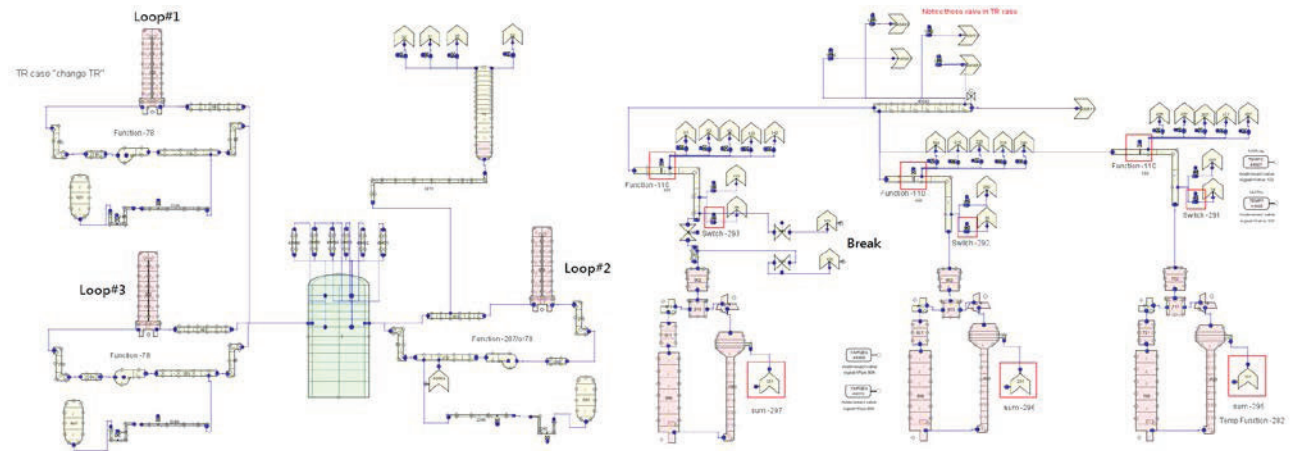


Figure 4. The TRACE model for Maanshan nuclear power plant with MSLB

3. METHODOLOGY

3.1. Mathematic model

The case was assumed as an incompressible, no heat source, and transient problem, the governing equations could be written as:

Continuity Equation:

$$\frac{\partial \rho}{\partial t} + \nabla \cdot (\rho \vec{U}) = \dot{m}$$

Momentum Equation:

$$\frac{\partial (\rho \vec{U})}{\partial t} + \nabla \cdot (\rho \vec{U} \vec{U}) = -\nabla P + \rho \vec{g} + \nabla \cdot (\mu \nabla \vec{U})$$

Energy Equation:

$$\frac{\partial}{\partial t} (\rho E) + \nabla \cdot (\vec{v} (\rho E + p)) = -\nabla \cdot (\sum_j h_j J_j) + S_h$$

3.2. Numerical model and simulation method

Under the high velocity flow and complex geometry conditions, the flow pattern and mixing phenomenon are significantly associated with the turbulence effect. Thus choosing an appropriate turbulence model by comparing with experiment data would assist us in the accuracy of flow behavior calculation. In this paper, three common turbulence models, Realizable $k-\varepsilon$ model, Standard $k-\omega$ model, and SST $k-\omega$ model, were selected to analyze the turbulence flow behavior. An applicable turbulence model was chose according to the result of verification between ROCOM experiment data and ROCOM CFD calculation.

SIMPLE-C (Semi-Implicit Method for Pressure-Linked Equations-Consistent) was employed for the pressure-velocity coupling in this case [8,9]. Momentum, volume fraction, turbulent kinetic energy, and turbulent dissipation rate of liquid phases were calculated by using the second order upwind scheme. The convergent residues of energy equation and momentum equation are less than 10^{-5} , and others are 10^{-3} .

3.3. Boundary conditions and treatment

The boundary conditions of steady-state of Maanshan CFD model were described at chapter 3.3.1. The TRACE analysis of MSLB event had been performed in Wang's research and was utilized as MSLB CFD model cold-leg inlet conditions in this paper [6].

3.3.1 Boundary conditions of steady-state

In Maanshan CFD model, the flow path was described as follows: a) Working flow was injected into downcomer via three cold-leg loops; b) The flow field of downcomer was slightly affected by neutron shield panels at inner-wall; c) In the lower-plenum, flow direction was changed due to the geometry of lower-plenum; d) Flow field was affected by complex structure and made non-uniform distribution in lower-plenum; e) Working flow arrived lower core plate, the outlet of CFD model. Boundary conditions of steady-state are based on NPP operating data and listed at table 2.

3.3.2 MSLB analysis

Table 3 shows the boundary conditions of major parameters in Maanshan TRACE model. In this model, the break area was 200% of main steam line cross-section area (double ended guillotine, DEG) and located at loop 3. In this analysis, the 0s-1000s was steady-state, and MSLB transient was occurred at 1000.01s. Figure 5 to Figure 8 show the results of MSLB TRACE calculation at cold-leg inlet. According to Fig. 5, power tripped when low pressure scram signal was obtained at 1000.05s. The curves of pressure and temperature of three loops show the similar trends (Fig.6 and 7). As the pressure reached 4240kPa, ACC injection was initiated to spray coolant water (at 1078s) via loop 2, and thus a higher mass flow rate in loop 2 occurs after ACC injection. The major sequence of Mannshan MSLB transient under TRACE prediction was shown in table 4. The results of TRACE model from 1000.01s to 1100s was utilized as the transient input-data of CFD model.

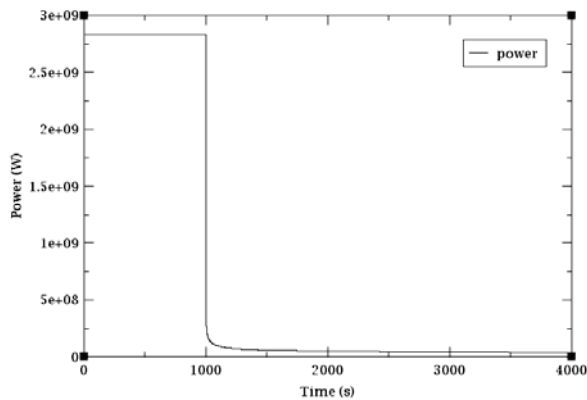


Figure 5. Power trips at 1000.05s

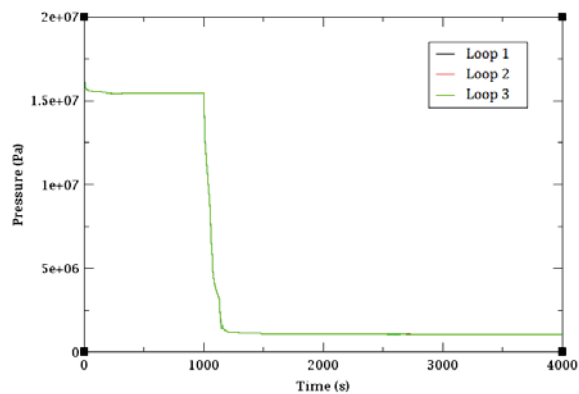


Figure 6. Inlet pressure of three cold-legs

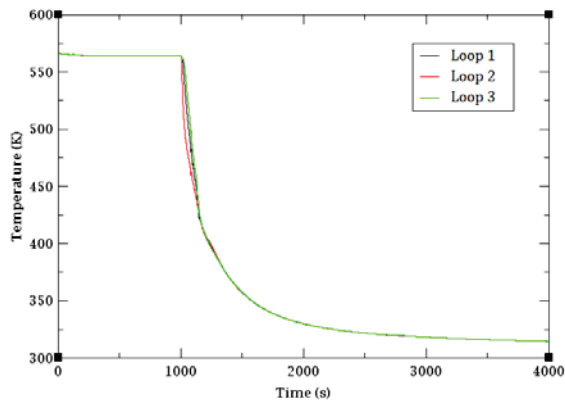


Figure 7. Inlet temperature of three cold-legs

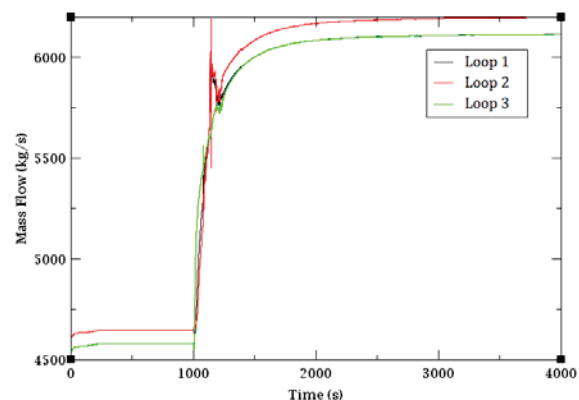


Figure 8. Inlet mass flow rate of three cold-legs

Table 2. Boundary conditions of Maanshan CFD model in normal operation

| Boundary conditions | Values |
|-----------------------------|---------------|
| Density(kg/m ³) | 740 |
| <u>Cold-leg</u> | |
| Mass flow rate (kg/s) | 4410.18 |
| Temperature (K) | 564 |

Table 3. Major parameters boundary conditions of Maanshan TRACE model

| Parameter | Values |
|---|-----------------------|
| Design pressure (MPa) | 15.6 |
| Maximum core power (MW) | 2775 |
| Primary system volume (m ³) | 2.15×10 ² |
| Number of loops | 3 |
| <u>Cold-leg</u> | |
| Inner diameter D (m) | 7.87×10 ⁻¹ |
| Length L (m) | 15.7 |
| L / √D (m ^{0.5}) | 17.69 |
| <u>Downcomer</u> | |
| Flow area (m ²) | 2.63 |
| Hydraulic diameter (m) | 4.8×10 ⁻¹ |
| <u>Core</u> | |
| Height (m) | 3.6 |
| Hydraulic diameter (m) | 1.22×10 ⁻² |
| Bypass area (m ²) | 1.54×10 ⁻² |
| <u>Hot-leg</u> | |
| Inner diameter, D (m) | 7.35×10 ⁻¹ |
| Length, L (m) | 7.28 |
| L / √D (m ^{0.5}) | 8.48 |
| <u>U-tube in one SG</u> | |
| Number | 5626 |
| Average length (m) | 16.85 |
| Inner diameter (mm) | 15.4 |
| Volume (m ³) | 18.44 |
| <u>Pressurizer</u> | |
| Volume (m ³) | 39.64 |
| Surge-line flow area (m ²) | 6.38×10 ⁻² |

Table 4. Major sequence of Mannshan MSLB in TRACE prediction

| Events | TRACE predicted (s) |
|-------------------------------------|----------------------------|
| Steady operation | 0 |
| Break occurred | 1000.01 |
| Low pressure scram signal (12.8MPa) | 1000.03 |
| Power trips | 1000.05 |
| MSIV closed | 1005 |
| ACC injection | 1078 |

4. RESULTS

Reliability of entire analysis process, including constructed model, meshing scheme, numerical method, and turbulence model, needs to be verified before starting the steady-state and transient-state calculations. Due to the real information of flow field in Maanshan vessel was unable to be obtained, a reliable experiment report was another solution. ROCOM report was selected for the verification of analysis process. ROCOM CFD model was constructed and calculated based on our analysis process. Comparisons between CFD and experiment results were verified the reliability of analysis process, and furthermore the same process was utilized in steady-state and transient-state calculations.

4.1 Verifications with ROCOM results

For verified the reliability of modeling and simulation method, ROCOM model was utilized in this study. Three common turbulence models were used in calculation embracing Realizable $k-\epsilon$, Standard $k-\omega$ and SST $k-\omega$. The CFD analysis results of circumference and radial direction in downcomer were obtained. The CFD results were compared with the results of ROCOM report.

4.1.1 Velocity distribution of circumference direction

As shown in Fig. 9, a similar curve with CFX simulation was obtained by Standard $k-\omega$ model result, but the result was slightly overvalued. The reasons might include that computational grid at cold-leg inlet was not precise enough, secondly flow at hot-leg region was affected by flow distribution at cold-leg (Fig. 10), and influence from flow resistance of wire-mesh sensors in downcomer was needed to consider.

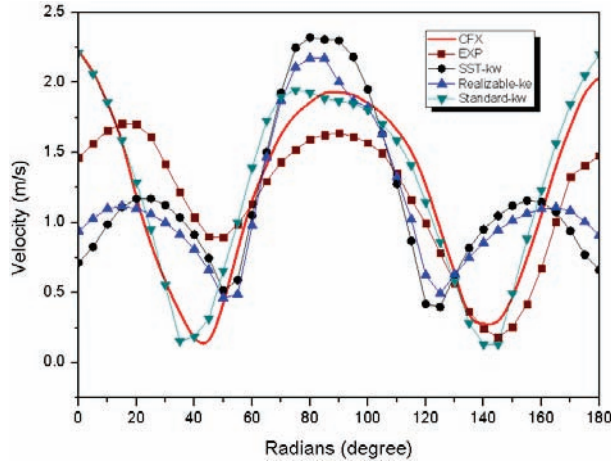


Figure 9. Circumference velocity distribution of different methods

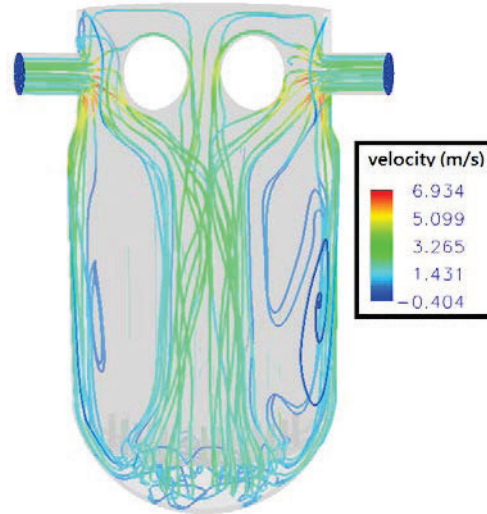


Figure 10. Streamline at hot-leg region of ROCOM CFD model

4.1.2 Velocity distribution of radial direction

The simulation results of velocity distribution at radial direction were also compared with ROCOM ROCOM experiment and CFX simulation, the effects of different turbulence model were considered as well. Width of downcomer was normalized for clear contradistinction, the function could be written as:

$$Y = \frac{y}{s}$$

When the y is distance from inside wall to measure point, the s is width in downcomer (Fig. 11).

Radial velocity distribution at 90° and 180° are shown in Fig. 12 and Fig. 13, respectively. The 90° flow field were located at downstream between two hot-leg flow region, velocity distribution was smaller than 180° because it was made via resultant vector from two further cold-leg loops.

As shown in figures, the approximate results were simulated by Standard $k-\omega$ model; there had slight deviation compared with experimental data near wall, it could be expected the conservative results of velocity gradient and heat transfer coefficient were obtained via Standard $k-\omega$ model and simulation method. Some characteristics in this verification are capsuled as follow:

- Since working flow is injected from cold-leg loops, velocity distribution of cold-leg is obviously higher than hot-leg region, hot-leg velocity distribution is constituted by resultant vector from two further cold-leg loops.
- Circumference velocity distribution at hot-leg region is affected through mesh quality; grid refinement will be proceeded at following simulation.
- Secondly flow is produced easily since the structure of hot-leg region.

According to above results, modeling, Standard $k-\omega$ turbulence model and numerical method setting used in ROCOM module were applied in Maanshan CFD module.

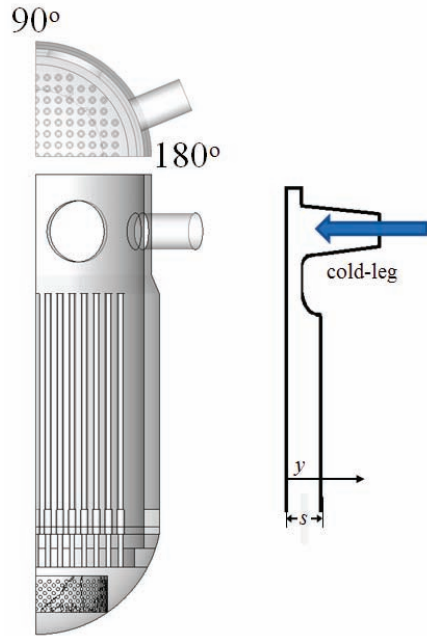


Figure 11. Normalized distance illustration

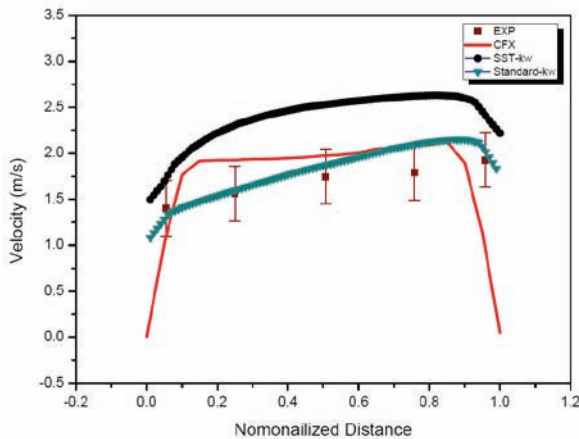


Figure 12. Radial velocity distribution of different methods at 90°

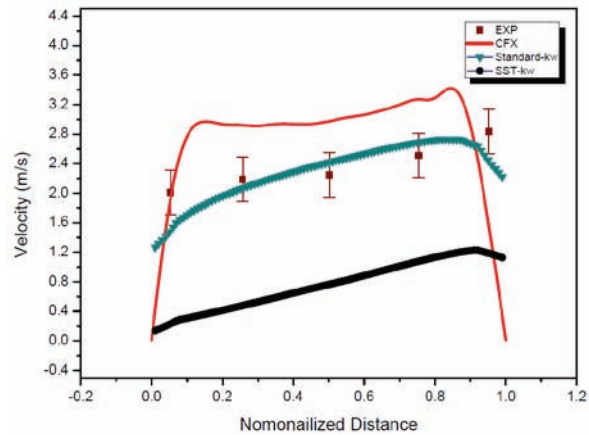


Figure 13. Radial velocity distribution of different methods at 180°

4.2 Analysis of steady-state in Maanshan CFD model

In this chapter, working flow was assumed isothermal flow during steady state simulation; flow path was the focus in results. As shown in Fig. 14, it was velocity profile at axial section of vessel model in normal operation. When working flow injected into vessel from cold-legs, the flow hit inside wall of vessel (point A), it was affected by flow area and flow direction, most of the flow went down to downcomer, rest of flow went up to top wall of vessel (point B) and made reverse flow. At point C, the flow was slower than point D due to neutron shield panels. In lower plenum, flow direction and model shape were major effects on working flow, most of water flowed to bottom along lower plenum wall, it crossed through tie-plates, pipes and core support, finally reached core bottom plate, a few water made turbulent flow and vortex at point E, there was slower flow near the tie-plates. At point F, flow hit core bottom plate and caused vortex.

Top profile in Fig. 14 was velocity distribution at horizontal section of downcomer and cold-legs; it located at point A of Fig 14. It showed that flow spread to both sides along radian of inside wall, some flow hit wall of hot-legs and caused reverse flow (point G). Figure 15 shows a clear stream line distribution in vessel model, stream lines spread along inside wall and most of them downed to downcomer, the rest struck top wall, then turned down along outside wall. As shown in Fig. 16, there had obvious velocity gradient at two locations between wall and lower tie-plate, which was made by turbulent flow.

4.3 Analysis of MSLB event in Maanshan CFD model

As the MSLB event occurred, the vessel temperature was reduced in short time. Figure 17 shows radial temperature distribution of different height at 1s, 78s and 100s, respectively. The locations of different height in Figure 17 had a larger variation of flow area or complex geometry, and the non-uniform mixing phenomenon was displayed in the region we interested. Moreover, the locations of different height had its corresponding point at Figure 14.

As shown in Fig. 17, an apparent temperature drop at 78s was found near the primary loop#2 in downcomer ($H=0m$, *point A*). The inference of phenomenon was the DEG at secondary loop#2. The non-uniform temperature distribution was occurred since the poor-mixing effect and limited space ($H=-2.15m$, *point C*), and the maximum temperature deviation in the downcomer was over 24K at 100s.

Non-uniform mixing still had no improvement in lower-plenum. Even there had bigger mixing space and vortex, the axial temperature distribution had the same trend along the height direction ($H=-6.93m$ and $H=-7.4m$, *point E*). Consequently, the radial temperature distribution forms a significantly non-uniform temperature distribution with maximum deviation 20K. It could be forecasted that an obviously temperature difference at the core inlet is inevitable.

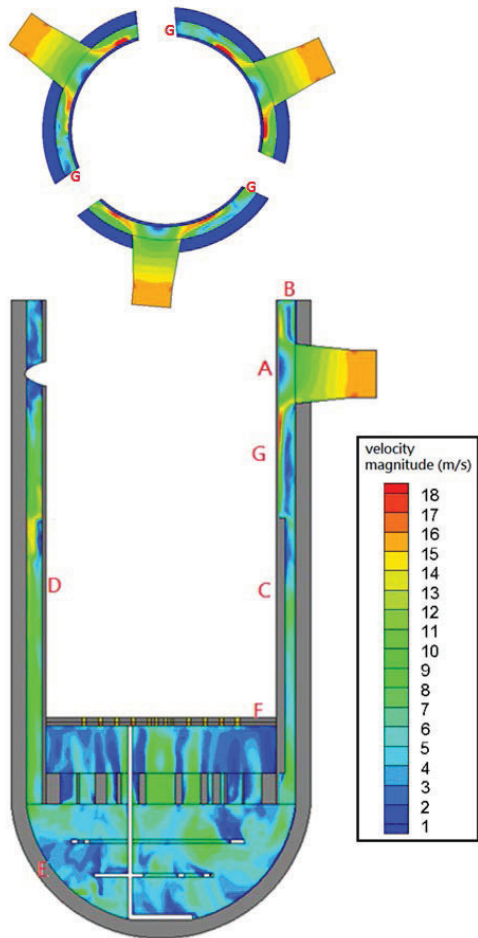


Figure 14. Velocity profile at axial and horizontal section of model

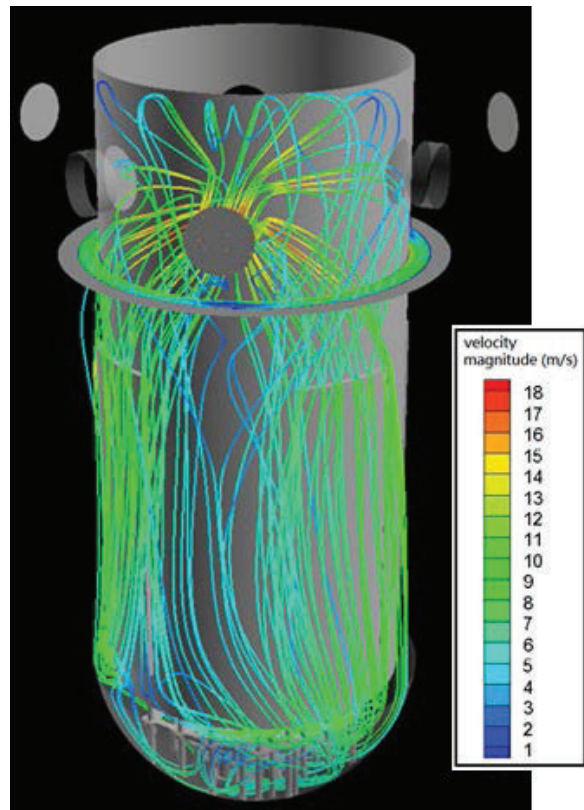


Figure 15. Stream line in Maanshan CFD model

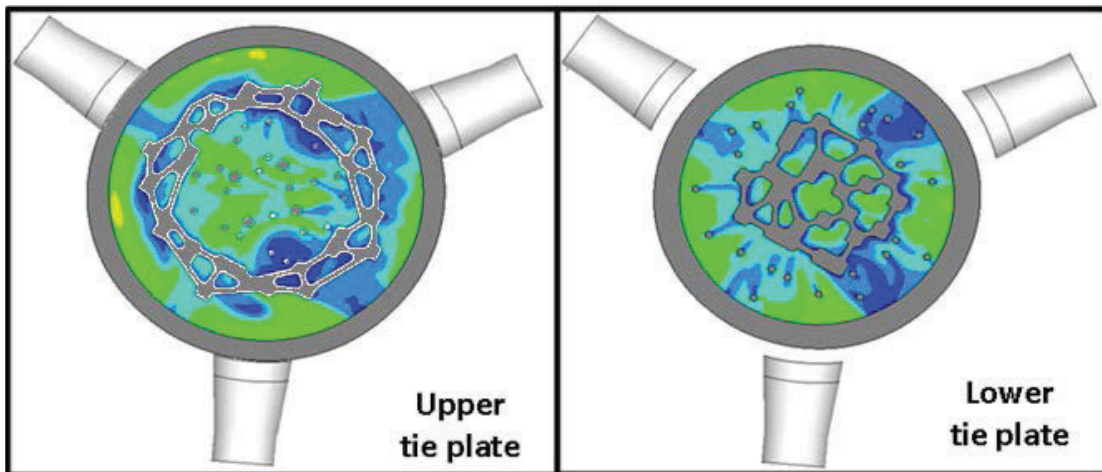


Figure 16. Velocity profile near the upper and lower tie-plates

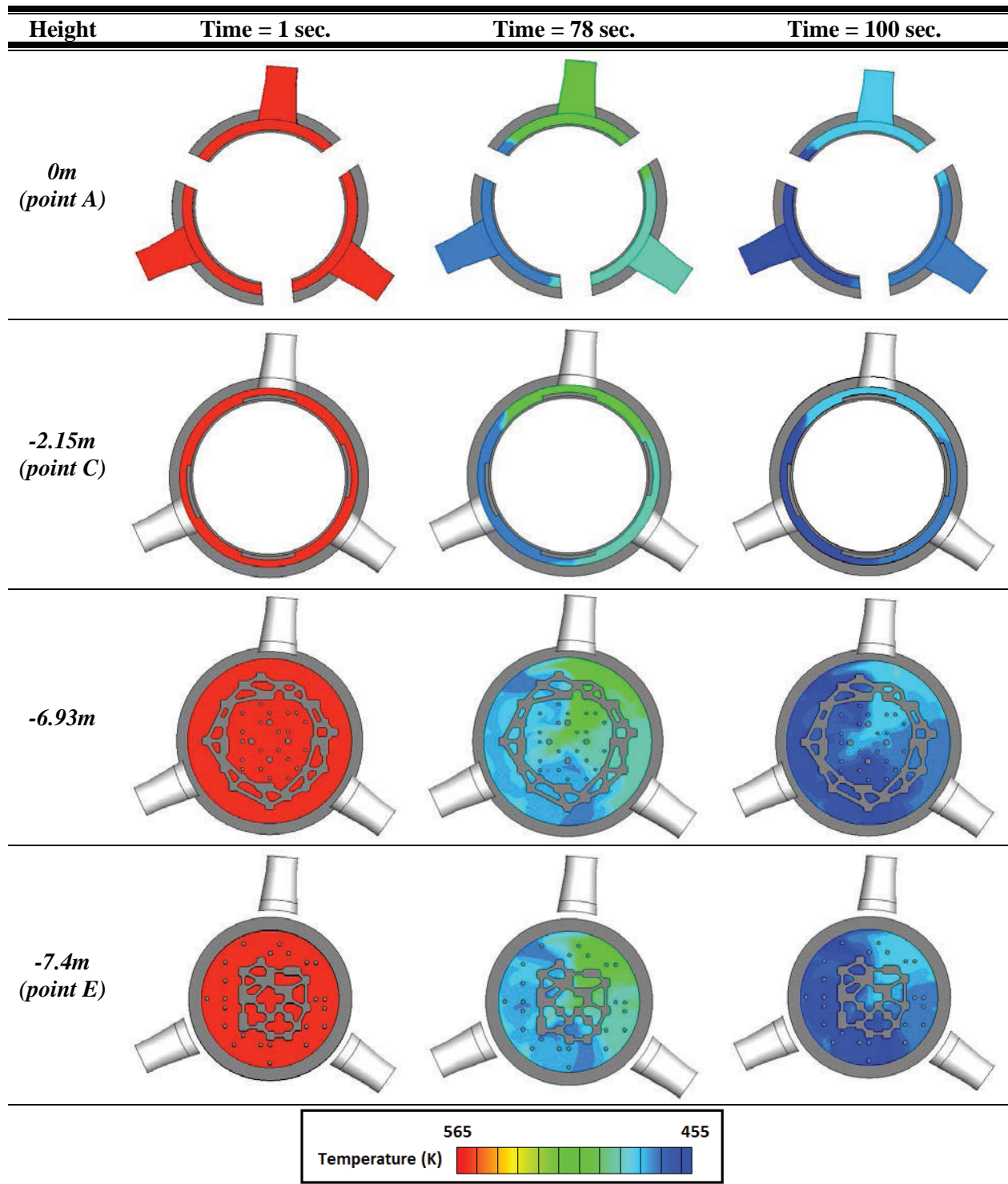


Figure 17. Radial temperature distribution of different height at 1s, 78s and 100s

5. CONCLUSIONS

In this study, a three-dimensional partial geometrical TRACE/CFD model of Maanshan PWR pressure vessel has been built to investigate the core flow behaviors and thermal hydraulic phenomena in downcomer and lower-plenum, and the model was employed to simulate steady-state conditions and the effects of MSLB transient event. Important settings of CFD model were first validated by benchmarking the ROCOM report. In order to provide sufficient transient boundary conditions of MSLB event for CFD simulations, the Maanshan TRACE model was coupled with the present CFD model. The flow fields inside the core under steady operations were obtained, and several vortexes caused by core geometries were found from the CFD results. In MSLB transient event, non-uniform temperature distributions were observed due to the limited space of downcomer and poor mixing of the core flow. The maximum temperature differences under the MSLB event can reach up to 24K and 20K in the downcomer and lower-plenum, respectively. This study successfully demonstrated a TRACE/CFD model for Maanshan PWR pressure vessel, and this methodology can be applied to nuclear reactor safety analysis for transient accident events.

REFERENCES

1. ANSYS, *FLUENT V12 Theoretical Manual*, ANSYS Inc. (2009).
2. T. Toppila, *The European project FLOMIX-R: Description of the experimental and numerical studies of flow distribution in the reactor primary circuit - Final report on WP 3*, Report FZR 431, Rossendorf, Dresden, Germany (2005).
3. U. Rohde, *The European project FLOMIX-R: Fluid mixing and flow distribution in the reactor circuit - Final summary report*, Report FZR 432, Rossendorf, Dresden, Germany (2005).
4. US Nuclear Regulatory Commission (USNRC), *TRACE V5.0 User Manual*, USNRC (2007).
5. Applied Programming Technology (APT), *Symbolic Nuclear Analysis Package (SNAP) User's Manual Report*, APT Inc. (2007).
6. Jong-Rong Wang, Hao-Tzu Lin, Yi-Hsiang Cheng, Wei-Chen Wang, Chunkuan Shih, "TRACE modeling and its verification using Maanshan PWR start-up tests", *Annals of Nuclear Energy* **36**(4), pp.527-536(2009).
7. M. di Marzo, D.E. Bessette, "Effect of depressurization on reactor vessel inventory in the absence of ECCS injection", *Nuclear Engineering and Design* **193**, pp.197-205 (1999).
8. S.V. Patankar, *Numerical Heat Transfer and Fluid Flow*, MC Graw-Hill, Washington (1980).
9. J.P. Van Doormal and G.D. Raithby, "Enhancements of the simple method for predicting incompressible fluid flows," *Numer. Heat Transf.* **7**, pp. 147-163 (1984).